APPLICATION OF DMD TO PIV VELOCITY FIELDS MEASURED IN FORCED JETS AND LIFTED FLAMES

S.S. ABDURAKIPOV[1,2], S.V. ALEKSEENKO[1,2], V.M. DULIN [1,2], D.M. MARKOVICH[1,2,c]

[1]Institute of Thermophysics, Siberian Branch of RAS, Novosibirsk, 630090, Russia
[2]Novosibirsk State University, Novosibirsk, 630090, Russia

[c]Corresponding author: Tel.: +7 383 3309040; Fax +7 383 3356684; Email: dmark@itp.nsc.ru

KEYWORDS:

Main subjects: large-scale vortices, round jet, lifted flame
Fluid: air, propane-air mixture
Visualization method(s): Particle Image Velocimetry, Dynamic Mode Decomposition
Other keywords: vortex dynamics, periodic forcing

ABSTRACT: The present work investigates the dynamics of coherent structures in a forced non-reacting jet and lifted propane-air flame by a Particle Image Velocimetry (PIV) technique and statistical analysis tool Dynamic Mode Decomposition (DMD). The PIV measurements were carried out with 1.1 kHz acquisition rate. Application of DMD to the measured set of the velocity fields provided information about frequencies, magnitude and shape of coherent structures. For the non-reacting jet, dynamics of the most powerful structures was associated with roll-up of vortices, their pairing and double pairing downstream. For the reacting flow, the frequency of vortices roll-up was observed to be about two times greater than that in the non-reacting jet, and no noticeable evidence of the vortex pairing was detected. When a periodic forcing in the range close to this frequency was applied, stability of the lifted flame increased, viz., blow-off and reattachment limits expanded significantly.

INTRODUCTION

It is well recognized that dynamics of large-scale vortices are crucial for heat and mass transfer process in turbulent shear flows, such as jets. It is also well known that periodical forcing is effective to control formation of vortices these flows. However, as it was shown in [1] vortex formation in a round forced jet can be rather distinctive (depending on frequency and amplitude of the forcing), since dynamics of the nonlinear open system is strongly affected by a feedback from downstream events of vortex roll-ups and pairings. Regarding jet flows with combustion, several papers (e.g., [2-6]) have outlined a significant role for large-scale vortices in stabilization mechanism of a lifted flame, especially when the flame is close to the nozzle (burner). For stabilization heights typically below 10 nozzle diameters, fuel and air before the flame front are not sufficiently premixed [7], and the stoichiometric iso-surface is significantly corrugated by large-scale vortices. The authors of [2] suggested that the flame spreads in the upstream direction along the outer periphery of large vortices (see also [4]). Thus, the vortices promote stabilization by transporting fuel to slowly co-flowing air, where velocity is much smaller than in the main jet flow. On the other hand, Watson et al. (e.g., [8]) paid attention to the fact that large-scale vortices also affect flame extinction process by stretching the front and leading to its local breaks. A significant role of large-scale vortices in stabilization mechanism of lifted flames has been confirmed by response of the flame when development of the vortices was controlled by external forcing (e.g., [9-11]), especially for small stabilization heights. In particular, by visualization of the flow in the fuel-rich diffusion propane-air lifted flame the authors of [9] observed that under periodic forcing the base of the flame front was the most likely located in the region of vortex roll-up and pairing, and it propagated along the outer boundary of the vortices. Besides, based on Particle Image Velocimetry (PIV) measurements of velocity fluctuations in the mixing layer upstream the fuel-rich premixed lifted flame and in the non-reacting flow Alekseenko et al. [12] assumed that in the former case, the flame could provide an additional forcing to the shear layer by generating acoustic noise. This possible 'feedback' can be significant for the mechanism of lifted flames stabilization for low nozzle-to-flame distances. Non-intrusive PIV technique can also provide insight on vortices role in the mechanism, since PIV allows to measure the instantaneous velocity fields and to analyze properties of large-scale vortices in the flow. A widely used technique for identifying coherent structures from velocity data is Proper Orthogonal Decomposition (POD) [13, 14]. The method determines the most energetic structures by diagonalizing the covariance matrix of velocity snapshots. However, the important

information about temporal evolution of coherent structures is commonly ignored. In [15], a DMD method for identifying coherent structures from PIV data was recently developed from Koopman analysis of nonlinear dynamical systems. The method provides information about scales and magnitude of coherent structures along with characteristic frequencies of their appearance. Thus, the present paper focuses on the study of large-scale eddies dynamics in a non-reacting jet and lifted fuel-rich flame by applying DMD to the data of carried out high-repetition PIV measurements. Additionally, to emphasize role of vortices in the flame stabilization process, a periodical fluctuations were superimposed to the initial velocity of the non-reacting and reacting flows.

EXPERIMENTAL SETUP

The measurements were carried out in an open combustion rig consisting of a burner, air fan, plenum chamber, flow seeding device, premixing chamber and section for the air and fuel (propane) flow rate control. The experiments were performed at the atmospheric pressure. The burner represented a profiled contraction nozzle described in [12] for the case of non-swirling flow. The exit diameter d of the nozzle was 15 mm. During the present study a non-reacting jet and lifted propane-air flame was investigated by a high-repetition PIV system. The Reynolds number Re_{air} (based on d and on flowrate and viscosity of the air) was fixed as 4 400. The equivalence ratio Φ of the propane-air mixture issuing from the burner was 2.5.

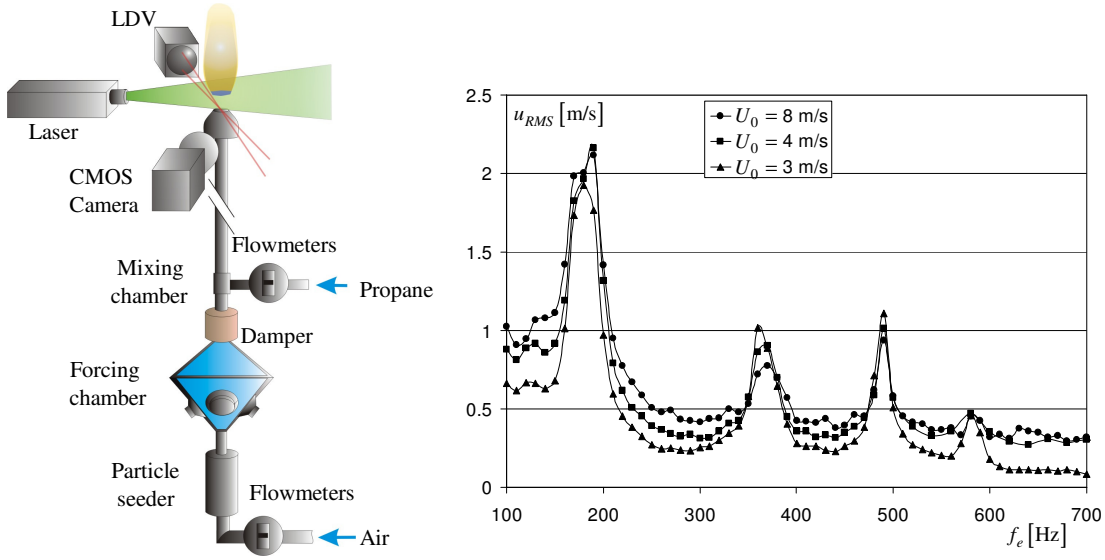

Fig. 1. Scheme of combustion rig and arrangement of measurement system (left). Root-mean-square values of the axial velocity fluctuations at nozzle exit, depending on frequency of sine voltage supplying loudspeakers (right).

To control formation of vortex structures, a system for periodic excitation was mounted at one and a half meter before the nozzle block. The forcing system represented a chamber with four loud speakers connected to an amplifier, function generator and electric power meter. During the PIV measurements, the normalized by d and U_0 frequency of the forcing, viz., the Strouhal number St, was St = 0.52 and St = 0.92. According to [1], the forcing at St = 0.52 corresponds to the range for which excitation amplifies vortices at the same frequency, while the forcing at St = 0.92 is associated also with a pairing event, and a significant modulation of perturbations takes place. Amplitude of the applied forcing was controlled by a Laser Doppler Velocimetry (LDV) probe for various frequencies and AC power of sine voltage applied to the system of loud speakers. Root-mean-square value u_{RMS} of the axial velocity fluctuations at the nozzle exit, which is related with the forcing amplitude, are shown in Fig. 1 (right) versus forcing frequency f_e. Three cases of the bulk velocity are considered: U_0 = 3.0, 4.0 and 8.0 meters per second. In all these cases, the electric power supplying the loudspeakers was fixed. One can observe a number of peaks (at about 185, 370, 490 and 580 Hz) associated with a resonance phenomenon of the combustion rig. The last three frequencies were associated with geometry of the nozzle

block, which is actually a Helmholtz resonator. High values of the velocity fluctuations in the range of the forcing frequencies below 160 Hz were associated with a thrasher function of the loudspeakers.

The used high-repetition PIV system was composed of a double-pulsed Nd:YLF Pegasus PIV laser (2×10 mJ at 2×1 000 Hz), PCO 1200HS CMOS camera and synchronizing device. A laser sheet, formed by the system of lenses, passed thru the central plane of the flow/flame and had a thickness of 0.8 mm in the measurement section. In order to provide PIV measurements, the main flow issuing from the nozzle was seeded by TiO_2 particles with the average diameter of one micrometer, and the ambient air was seeded by a fog. The camera was equipped with a narrow-bandwidth optical filter admitting the emission of the lasers and suppressing the radiation of the flame. The system was operated by a computer with "ActualFlow" software. The delay between illuminations of tracer particles for each image pair was 70 μs. Time step between the pairs was 900 μs resulting to the acquisition frequency of about 1.1 kHz. Each captured 12 bit image pair was pre-processed by subtracting 80% of the intensity that was averaged over the whole image set. Velocity fields were calculated by an iterative cross-correlation algorithm with an image continuous shift and deformation [16]. Size of a final interrogation area was 32×32 pixels (corresponded to about 2.2×2.2 mm). 75% overlap rate between the interrogation areas was used to increase robustness of validation procedures (e.g., 5×5 moving average filter) used between iterations of the cross-correlation algorithm. The instantaneous velocity vectors after the final iteration were validated by using a signal-to-noise criterion for cross-correlation maxima and by an adaptive median filter from [17]. For each flow case, 6 00 instantaneous velocity fields were measured. Based on the estimated velocity fields, the spatial distributions of the mean velocity and components of turbulent kinetic energy (TKE) were calculated. A DMD approach was applied to the set in order to analyze the dominant frequencies and scales of coherent structures both in reacting and non-reacting flows.

A temporal sequence of N PIV velocity fields $\boldsymbol{u}_i$, with a constant time interval Δt can be written as a matrix $V_1^N = \{\boldsymbol{u}_1, \boldsymbol{u}_2, \boldsymbol{u}_3, \ldots, \boldsymbol{u}_N\}$. In general DMD is a decomposition of data ensemble into finite series of complex Fourier harmonics, i.e., products of spatial complex basis functions $\boldsymbol{\phi}_n$ with time-dependent complex coefficients b_k (amplitudes):

$$\boldsymbol{u}(x,t_i) = \sum_{k=1}^{N-1} b_k(t_i)\boldsymbol{\phi}_k(x) = \sum_{k=1}^{N-1} e^{(\omega_r^k + i\omega_i^k)t_i}\boldsymbol{\phi}_k(x) \tag{1}$$

The problem can be solved by finding global Eigen modes of linear mapping matrix $\boldsymbol{A}$:

$$\boldsymbol{u}_{i+1} = e^{\tilde{A}\Delta t}\boldsymbol{u}_i = A\boldsymbol{u}_i \tag{2}$$

According to Schmid [15], where the idea underlying the Arnoldi method was used, a low-dimensional approximation S of A can be obtained by representing the last snapshot from the sequence as a linear combination of the previous ones:

$$\boldsymbol{u}_N = a_1\boldsymbol{u}_1 + a_2\boldsymbol{u}_2 + \ldots + a_{N-1}\boldsymbol{u}_{N-1} = V_1^N\boldsymbol{a} + \boldsymbol{r} \tag{3}$$

$$\begin{cases} V_2^N = AV_1^{N-1} = \{A\boldsymbol{u}_1, A\boldsymbol{u}_2, A\boldsymbol{u}_3, \ldots, A\boldsymbol{u}_{N-1}\} \\ V_2^N = \{\boldsymbol{u}_2, \boldsymbol{u}_3, \ldots, \boldsymbol{u}_N\} = \{\boldsymbol{u}_2, \boldsymbol{u}_3, \ldots, V_1^N\boldsymbol{a} + \boldsymbol{r}\} \end{cases} \Rightarrow V_2^N = AV_1^{N-1} = V_1^{N-1}S + \boldsymbol{r}\boldsymbol{e}^T \tag{4}$$

Here S is a low-dimensional companion matrix of A, $\boldsymbol{r}$ is the residual vector and $\boldsymbol{e}^T$ is the (N-1)th unit vector. The least-squares problem for the low-dimensional matrix S (i.e., for minimization of $\|\boldsymbol{r}\|$) can be solved by using a QR-decomposition:

$$V_1^{N-1} = QR \Rightarrow S = R^{-1}Q^TV_2^N \tag{5}$$

As the eigenvalues of S approximate some of the eigenvalues of A [15], a corresponding eigenproblem of S is solved:

$$S\boldsymbol{y}_k = \mu_k\boldsymbol{y}_k \tag{6}$$

The spatial dynamic modes $\boldsymbol{\phi}_k$ can be calculated by projecting the velocity data V_1^{N-1} onto the associated eigenvector $\boldsymbol{y}_i$:

$$\boldsymbol{\phi}_k = V_1^{N-1}\boldsymbol{y}_k \tag{7}$$

In general, the eigenvalues and the eigenvectors are complex numbers. Frequency ω_i and growth rate ω_r of a corresponding dynamic mode is obtained by the logarithmic mapping (8).

$$\omega_k = \frac{Ln(\mu_k)}{2\pi\Delta t} = \omega_r^k + i\omega_i^k \tag{8}$$

The obtained dynamic modes in (1) are non-orthogonal. They can be sorted by either by frequency ω_i, L_2-norm (coherence measure) of the mode or growth rate ω_r. To eliminate from the further analysis modes with a very small energy, which were generally associated with noise, dynamic modes $\boldsymbol{\phi}_k$ were projected onto a truncated POD basis (the

first ten modes) of $\boldsymbol{u}_i$. Coherence measure was estimated by finding the norm of the resulting vector. Since stationary turbulent flows were studied in the present paper, the obtained DMD modes corresponded mainly to the case $\omega_r \leq 0$. The modes with a fast decay rate (viz., $\omega_r << 0$) were excluded from the analysis.

Thereby the application of DMD to the ensembles of high-repetition PIV data provided a set of eigenvalues (spectrum) and the corresponding eigenvectors (dynamic modes), which contained valuable information about dynamic processes in the original data sequences. The decomposition allowed to estimate dominant frequencies of velocity pulsations in the turbulent flows and to analyze shape of the associated coherent structures. Temporal evolution and interaction of large-scale vortices in the studied flow was also analyzed from a low-order model (1) based on few dominant dynamic modes and the mean velocity field.

RESULTS

To emphasize role of large-scale vortices in stabilization mechanism of the studied lifted flame, visualized of the external periodical forcing effect on the flame was carried out prior to the PIV measurements. Fig. 2a shows blow-off curves on a Re-Φ diagram for the unforced (red line) and forced with frequency 300 Hz (blue line) lifted propane-air flame. In particular, the forcing in a range around 300 Hz increased the blow-off limit the most efficiently for the tested range of bulk velocities from 2 to 6 m/s. The forcing also delayed the reattachment event. Presented in the right part of Fig. 1 photographs correspond to the cases of the lifted flame for Re_{air} = 4 400, U_0 = 5.0 m/s, Φ = 2.5 without forcing (u_{RMS} was below 4% of U_0) and forced at f_e = 170 and 300 Hz (by selecting proper AC voltage, u_{RMS} in both cases was fixed as 10% of U_0). Remarkable that the forcing at 170 Hz (i.e., at St = 0.52 for U_0 = 5.0 m/s) did not noticeable increase the blow-off limit. In other words, the lowest value of Φ for the stable combustion for the flame forced at St = 0.52 was same as in the unforced flame. In contrast, the forcing 300 Hz (St = 0.92 for U_0 = 5.0 m/s) resulted in a decrease of the flame stabilization height (from 1.3*d* to 0.6*d*, as it was determined from additional measurements of CH* chemiluminescence signal) and resulted in a wider range of Φ (towards leaner flames) for the stable combustion without blow-off.

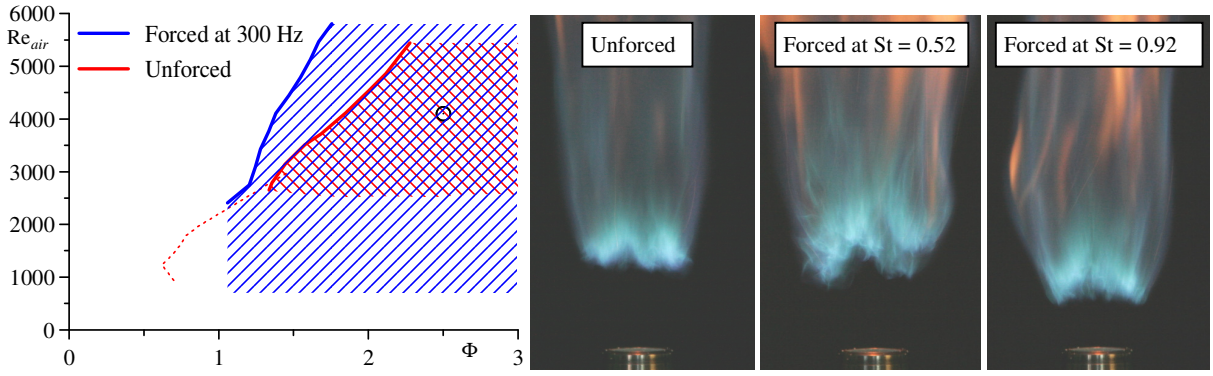

Fig. 2 The blow-off curves and domains of stable combustion for a propane-air lifted flame (- unforced; - forced at 300 Hz) (left). Photographs of lifted flame at Re_{air} = 4 400. U_0 = 5.0 m/s, Φ = 2.5 (right)

Fig. 3 shows the spatial distributions of the normalized mean velocity **U** measured for the unforced and forced lifted flames in Fig. 2. Fig. 3 also contains the distributions of the radial component of TKE to characterize intensity of the velocity fluctuations in the flows. The flow structure of the each flame is compared to that of the non-reacting jet. For the cases without combustion the forcing did not sufficiently affect **U**, but provided to a significant increase of the radial velocity fluctuations in the mixing layer due to promoting formation of large-scale vortices. The forcing at St =0.5 had much larger effect in comparison to St =0.92 since it was in the range of "preferable" frequency for a round jet: St = 0.3-0.6. According to the distributions of **U**, the presence of combustion resulted in a deflection of the flow after the lame onset towards the positive radial direction and led to an increase of the velocity magnitude due to the thermal expansion of the fluid after the chemical reaction. By comparing the radial component of TKE for the unforced non-reacting and reacting flows, significantly larger values can be observed in the latter case for the region between the

flame and the nozzle. As it was supposed in [12], this could be due an additional forcing to the shear layer from acoustic noise generated by the flame. In general, for all reacting cases values of $\langle v^2 \rangle$ before the flame onset appear to be greater than those for the corresponding non-reacting flow. Downstream, the flame onset, magnitude of the velocity fluctuations decreased due to the growth of the fluid temperature. Another feature that corresponded to the reacting cases is significant radial velocity fluctuations in the region for $r/d > 0.7$ after the flame base, where secondary shear layer is formed between the hot products and the ambient air.

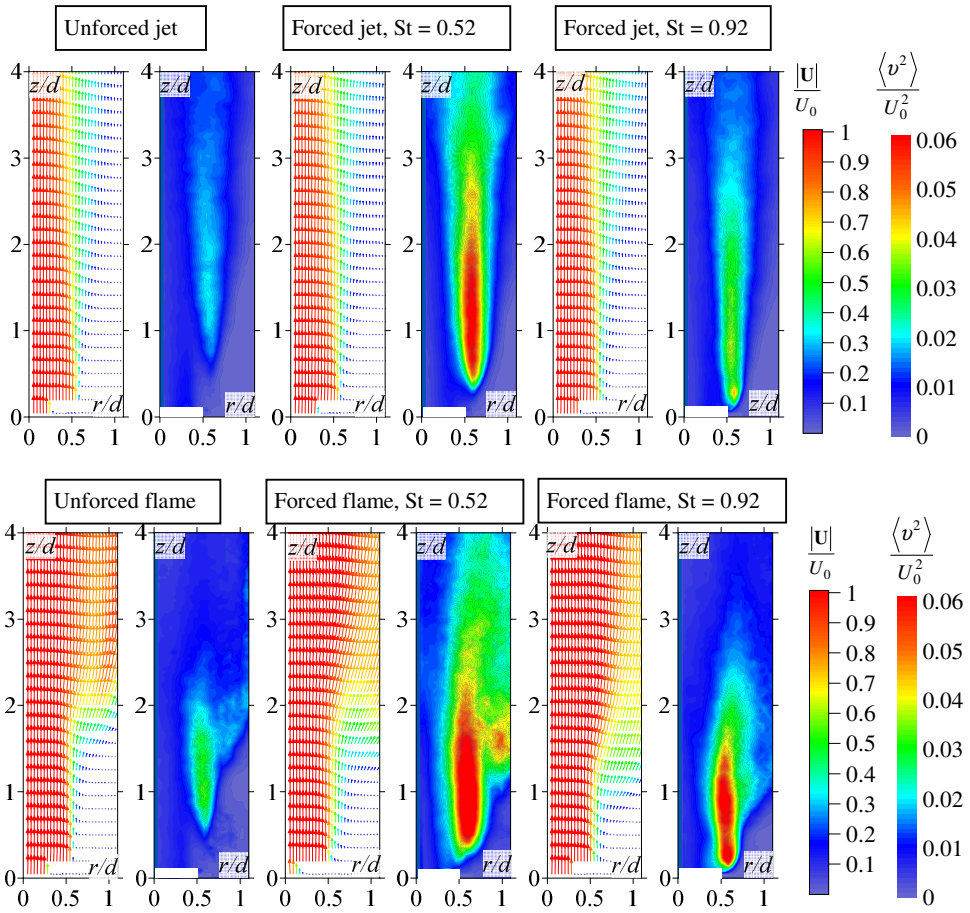

Fig. 3 Distributions of the mean velocity and radial component of turbulent kinetic energy for a non-reacting jet and lifted flame with and without forcing. Re_{air} = 4 400, U_0 = 5.0 m/s, Φ = 2.5.

Fig. 4 depicts coherence measure (L_2-norm of $\boldsymbol{\phi}_k$ projected on ten the most coherent modes of POD basis) of the dynamic modes as a function of frequency ω_i. DMD spectra are symmetric about the frequency ω_i. = 0 because the decomposed data are real. Negative ω_i corresponds to mode $\boldsymbol{\phi}_k$ with the same real part, but negative imaginary part of the mode for $-\omega_i$. Thus, the spectra are displayed for $\omega_i > 0$ only. To demonstrate spatial structure of the dominant dynamic modes for the studied flows, the radial or axial components of their real and imaginary parts are presented in Fig. 5. As can be seen, the real and imaginary parts differ in $\pi/2$ phase shift. In general, as the mixing layer is convectively unstable, the lower frequency of the pulsations is, the larger coherent structure is associated with them. The exception is for the unforced lifted flame, where the dynamic mode at 2 Hz is expected to be caused by a movement of the lifted flame base during the observation period. According to the DMD spectra and dynamic modes for the unforced jet, three main harmonics were the most dominant in the studied domain of the flow: fundamental frequency of vortices roll-up f_0 (St = 0.4), sub-harmonic $f_0/2$ of the vortex pairing and quarter harmonic $f_0/4$ of double pairing event. Thus, interactions at sub-harmonics resulted in a modulation in amplitude of the perturbations developed

in the shear layer for the whole studied region. For the non-reacting jet with periodic forcing at St = 0.52, a strong peak was detected at the fundamental frequency f_0 along with the secondary peak for the doubled frequency. For the case St = 0.92, several lower harmonics were significant in the DMD spectrum of the non-reacting jet: fundamental peak f_0, sub-harmonic $f_0/2$ and two sub frequencies with $f_1 + f_2 = f_0/2$. They are expected to correspond to a modulation of amplitude of rolling-up vortices and coherent structures after the vortices pairing (i.e., irregular pairing took place). For the both cases of forcing, the dynamic modes of the fundamental frequency f_0 show formation of strong vortex structures just after the nozzle rim. The structures had a large amplitude until z/d approximately 3.5 and 2.5 for St = 0.52 and St = 0.92, respectively. As can bee seen for the case St = 0.92, pulsations at the main harmonic (f_0) and sub-harmonic ($f_0/2$) were dominated in different regions of the mixing layer. When the main harmonic degenerated, the sub-harmonic grew. As it was mentioned, the nixed frequencies ($f_1 + f_2 = f_0/2$) were concluded to be associated with a mutual modulation of amplitudes of the fluctuations at the fundamental and sub-harmonic frequencies due to the presence of feedback in the convectively unstable jet flow [1].

For the unforced propane-air lifted flame, the DMD analysis revealed the presence of three pronounced peaks at 2, 17, 308 Hz among a band of other frequencies. The first frequency (2 Hz) was related to a shift of the flame base during the measurements, the second one corresponds to large-scale fluctuations in the mixing layer after the flame front and could be connected with oscillations of heat release. The third frequency 308 Hz was associated with coherent structures formed in the mixing layer upstream the flame front. Thus, the presence of combustion shifted the frequency of vortices roll-up towards the higher value, viz., from St = 0.4 to 0.92. For the flame forced at St = 0.52 and St =0.92, along with the intensive vortex structures rolling-up at the forcing frequency, low-amplitude pulsations were also present in the flow for the frequency below 20 Hz. In general, based on the visualization (see Fig. 2) and DMD analysis for the reacting flow case without forcing and with forcing at St = 0.92, it can be argued that the excitation promoted formation of the vortices at the "natural" frequency of the reacting flow. As a consequence, the flame stability increased due to the enhanced mixing upstream. However these experimental observations require a more detailed investigation.

Depicted in Fig. 6 the low-order model (reconstruction) built from the superposition of relevant dynamic modes (the modes are marked by open circles in Fig. 4) to the mean velocity field allowed to approximate flow dynamics associated with the most coherent structures. Rainbow colorscale corresponds to the radial component of the reconstructed velocity field. Vortex structures in the figures are visualized by a positive value of swirling strength criterion (see [18]). As can be seen, the model approximates not only temporal evolution, but also interaction of large-scale coherent structures in the mixing layer of the non-reacting and reacting jets. Thus, the reconstruction captures the process of vortices pairing in the unforced and forced at St = 0.92 non-reacting flows. For example, merging of the forced vortices (marked by triangles) and formation of a larger structure at the distance $z/d \approx 2.5$ is demonstrated for the latter case. The reconstruction based on three dominant dynamic modes (2, 17, 308 Hz) and the mean velocity field for the unforced reacting case reflects the process of interaction between the vortices and the flame front. In particular, intensity of the vortex has decreased after the fluid expansion. For the rest cases (forced non-reacting jet at St = 0.52; forced flame at St = 0.52 and St = 0.92) only one the most coherent dynamic mode, associated with forcing frequency, was used in the low-order model. Sequences of reconstructed velocity fields for these cases show a periodical rolling-up, convection and decaying of the vortex structures, during the excitation. Remarkable, that in addition to the excited vortex structures, the reconstruction also reveals the presence of secondary vortices for the forced reacting cases. The secondary vortices were just after the onset of the lifted flame: near z/d = 1.25 and 0.75 for the cases St = 0.52 and St = 0.92, respectively. The secondary vortex can also be detected near z/d = 1.5 for the unforced flame. It is remarkable that the authors of [11] consider secondary vortices to even more important for stabilization of the lifted flame than the primary vortex rings.

CONCLUSIONS

The paper describes the results of high-repetition PIV measurements in a turbulent non-reacting jet and lifted propane-air flame without forcing and under periodic forcing at two frequencies, viz., St = 0.52 and St = 0.92. The set of the measured instantaneous velocity fields was processed by a DMD algorithm. Obtained DMD spectra provided dominant frequencies of velocity fluctuations in the flows. Dynamic modes of the decomposition contained information about scale and magnitude of the corresponding coherent structures along with the regions of flows where these structures emerged. For the unforced non-reacting jet the decomposition revealed fundamental frequency of vortices roll-up (St = 0.4), sub-harmonic of the vortex pairing and quarter harmonic of the double pairing event. For the jet flow forced at

St = 0.92, non-linear interaction of different harmonics was detected from the DMD spectrum and dynamic modes: modulation of amplitude of the vortices roll-up and pairing process took place corresponding to an irregular pairing phenomenon.
For the unforced reacting case, the frequency of vortices roll-up was found to be shifted towards a higher value, viz., to St = 0.93. When the forcing at this frequency was applied, an increase of the lifted flame stability took place: the blow-off limit (bounding the lowest equivalence ratio for the stable flame) has expanded in comparison to the unforced flame. Based on DMD analysis of the measured PIV data it can be concluded that the observed increase of the lifted flame stability was associated with a resonant amplification of a feedback from the flame to the upstream shear layer. The forcing promoted the rolling-up of the "natural" vortices which determined mixing process before the flame front.

ACKNOWLEDGEMENTS

This work was performed under funding by the Government of Russian Federation (Grant No. 11.G34.31.0046), Federal Oriented Programs “Scientific, research and educational cadres for innovative Russia” for 2009–2013 and “Research and engineering in priority directions for development of Russia's scientific-technological complex" for 2007–2013). The research was also supported by the European Community’s Seventh Framework programme (FP7/2007-2013, grant agreement No.265695) and by the Russian Foundation for Basic Research (grant N 11-08-00985). The authors kindly acknowledge Prof. K. Hanjalic for fruitful discussions.

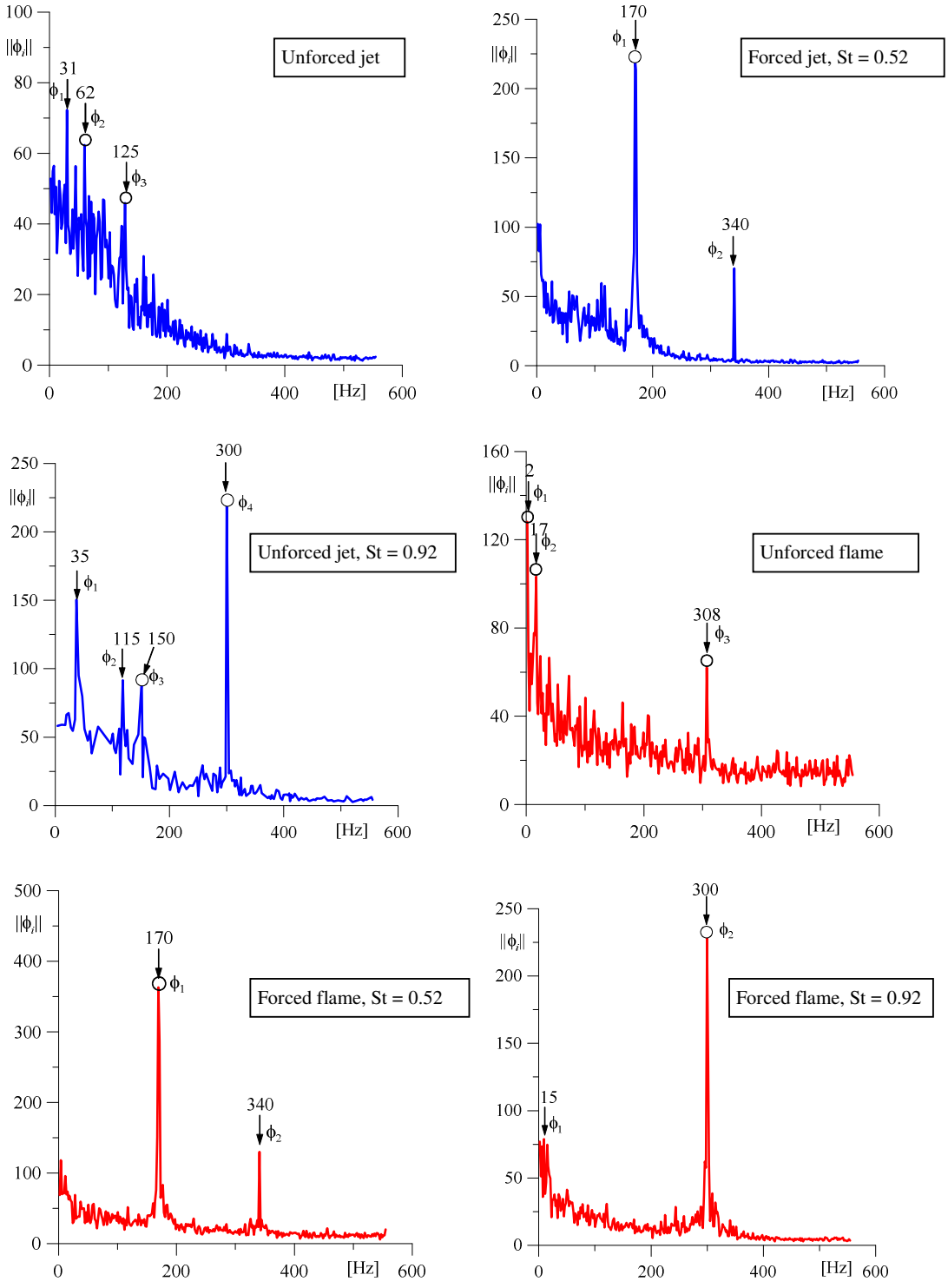

Fig. 4 Spectra of dynamic modes for different flow regimes. Re_{air} = 4 400, U_0 = 5.0 m/s, Φ = 2.5. The modes marked by arrows and by open circles are presented in Fig. 5 and used for reconstruction in Fig. 6, respectively.

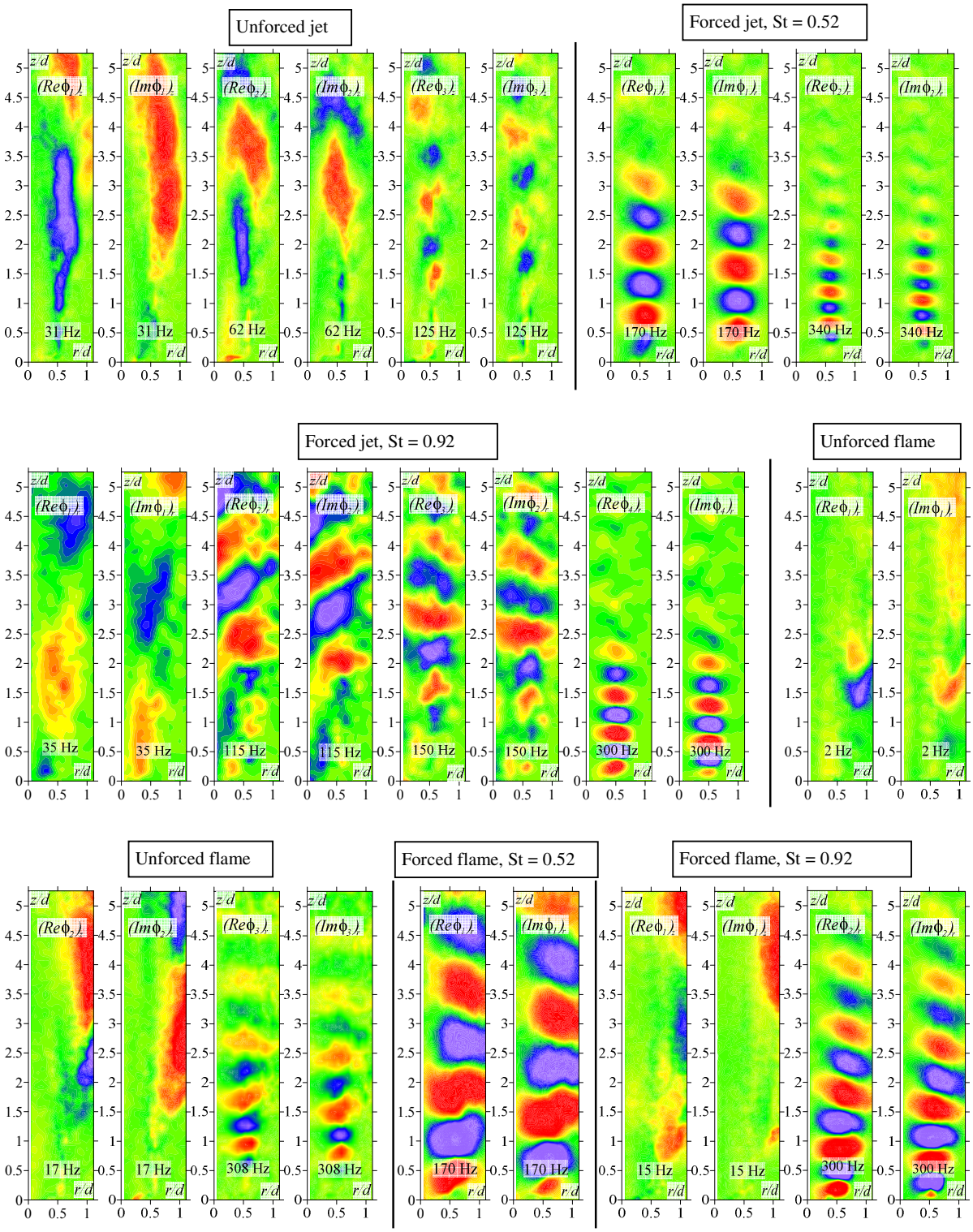

Fig. 5 Spatial distributions of the radial and axial components of dominant dynamic modes (real and imaginary parts) for different flow regimes. Re_{air} = 4 400, U_0 = 5.0 m/s, Φ = 2.5.

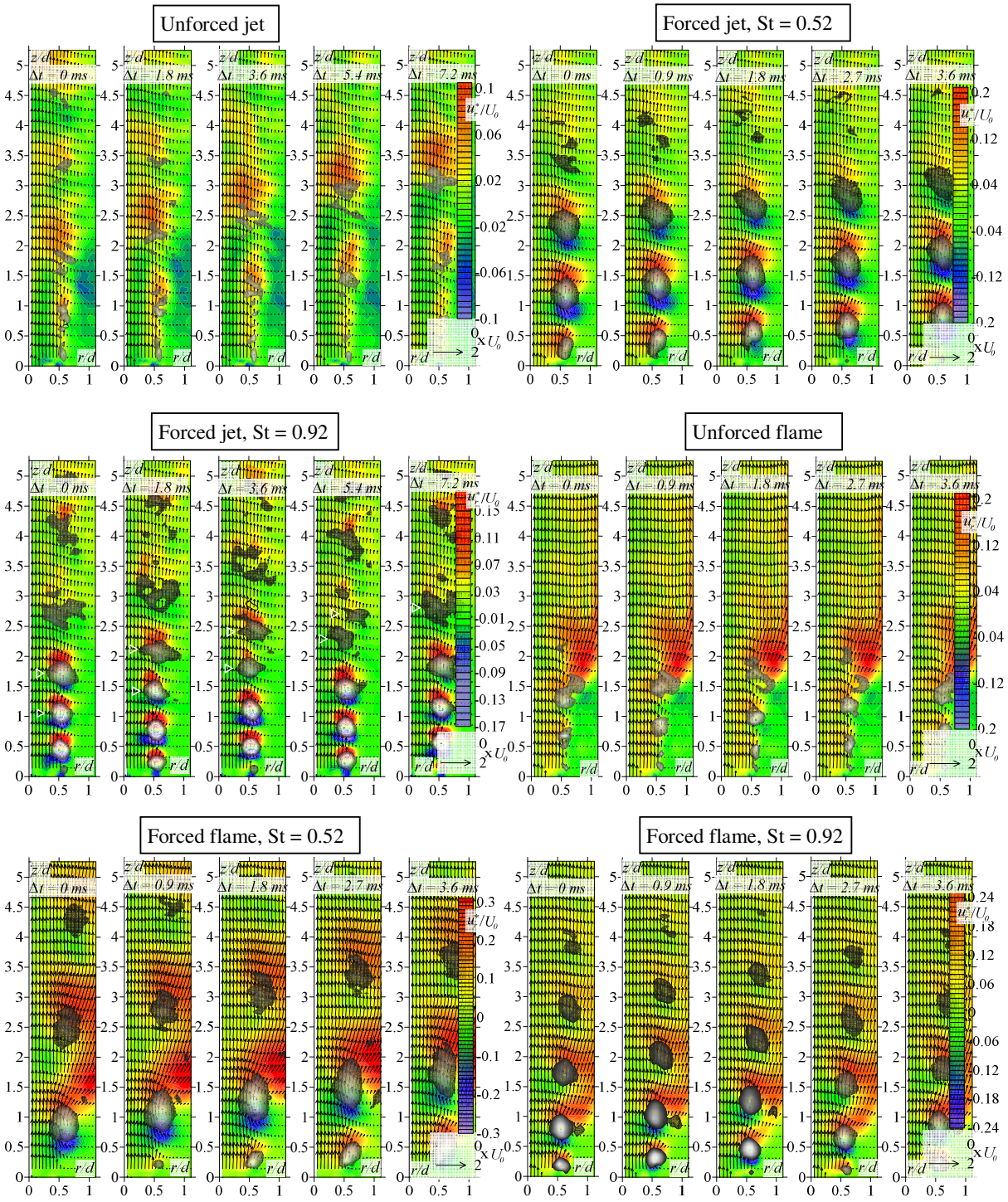

Fig. 6 Low-order reconstruction of a sequence of five instantaneous velocity fields for studied flow regimes. Color map corresponds to the radial component of the reconstruction. Partially transparent grayscale layer shows swirling strength [18]. Re_{air} = 4 400, U_0 = 5.0 m/s, Φ = 2.5.

References

1. Broze G., Hussain F. *Transitions to chaos in a forced jet: intermittency, tangent bifurcations and hysteresis.* J. Fluid Mech. 1996, **311**, pp. 37-71.
2. Broadwell J.E., Dahm W.-J.A., Mungal M.G. *Blowout of turbulent diffusion flames. Proc. of 28th Symp. (Int.) on Combust*. 1984, pp. 303-310.
3. Miake-Lye R.C., Hammer J.A. *Lifted Turbulent Jet Flames: A Stability Criterion Based on the Jet Large-Scale Structure*. Proc. Combust. Inst. 1988, **22**, pp. 817-823.
4. Kaplan C.R., Oran E.S., Baek S. *Stabilization Mechanism of Lifted Jet Diffusion Flames*. Proc. Combust. Inst. 1994, **25**, pp. 1183-1192.
5. Burgess C.P., Lawn C.J. *The premixture model of turbulent burning to describe lifted jet flames.* Combust. Flame. 1999, **119**, pp. 95-108.
6. Upatnieks A. et al. *Liftoff on turbulent jet flames-assessment of edge/flame and other concepts using cinema-PIV*. Combust. Flame. 2004, **138**. pp. 252-272.
7. Lawn C.J. *Lifted flames on fuel jets in co-flowing air*. Progr. Energy Combusti. Sci. 2009, **35**, pp. 1-30.
8. Watson K.A., Lyons K.M., Donbar J.M., Carter C.D. *Scalar and Velocity Field Measurements in a Lifted CH_4-Air Diffusion Flame*. Combust. Flame. 1999, **117**, pp. 257-271.
9. Lin C.-K., Jeng M.-S., Yei-Chin Chao Y.-C. *The stabilization mechanism of the lifted jet diffusion flame in the hysteresis region*. Exp. Fluids. 1993, **14**, pp. 353-365.
10. Chao Y.-C., Wu C.-Y., Yuan T. and Cheng, T.-S. *Stabilization process of a lifted flame tuned by acoustic excitation*. Combust. Sci. Tech. 2002, **174**, pp. 87.
11. Baillot F., Demare D. *Responses of a lifted non-premixed flame to acoustic forcing. Part2.* Combust. Sci. Technol. 2007, **179**, pp. 905–932.
12. Alekseenko S.V. et al. *Flow structure of swirling turbulent propane flames*. Flow Turbul. Combust. 2011, **87**, pp. 569-595.
13. Sirovich L. *Turbulence and the dynamics of coherent structures, parts i-iii*. Quart. J. Appl. Math. 1987, **45**(3), pp. 561-90.
14. Holmes P., Lumley J.L., Berkooz G. *Turbulence, coherent structures, dynamical systems and symmetry.* University press, Cambridge, 1996.
15. Schmid P.J. *Dynamic mode decomposition of numerical and experimental data*. J. Fluid Mech. 2010, **656**, pp. 5-28.
16. Scarano F. *Iterative image deformation methods in PIV*. Meas. Sci. Technol. 2002, **13**, pp. 1–19.
17. Westerweel J., Scarano F. *Universal outlier detection for PIV data*. Exp. Fluids. 2005, **39**, pp. 1096–1100.
18. Zhou J., Adrian R. J., Balachandar S., Kendall T. M. *Mechanisms for generating coherent packets of hairpin vortices in channel flow*. J. Fluid Mech. 1999, **387**, pp. 353-396.